Journal of Macromolecular Science, Part A
Publication details, including instructions for authors and subscription information:
http://www.informaworld.com/smpp/title~content=t713597274

Miscibility and Biodegradation Behavior of Melt-Processed Blends of Bacterial Poly(3-Hydroxybutyrate) with Poly(Epichlorohydrin)

Lara Finelli[ab]; Beatrice Sarti[ab]; Mariastella Scandola[ab]
[a] Dipartimento di Chimica "G. Ciamician", dell'Università di Bologna, [b] Centro di Studio per la Fisica delle Macromolecole del C.N.R., Bologna, Italy

To cite this Article Finelli, Lara , Sarti, Beatrice and Scandola, Mariastella(1997) 'Miscibility and Biodegradation Behavior of Melt-Processed Blends of Bacterial Poly(3-Hydroxybutyrate) with Poly(Epichlorohydrin)', Journal of Macromolecular Science, Part A, 34: 1, 13 — 33

To link to this Article: DOI: 10.1080/10601329708014931

URL: http://dx.doi.org/10.1080/10601329708014931

J.M.S.—PURE APPL. CHEM., A34(1), pp. 13–33 (1997)

MISCIBILITY AND BIODEGRADATION BEHAVIOR OF MELT-PROCESSED BLENDS OF BACTERIAL POLY(3-HYDROXYBUTYRATE) WITH POLY(EPICHLOROHYDRIN)

LARA FINELLI, BEATRICE SARTI, and
MARIASTELLA SCANDOLA*

Dipartimento di Chimica "G. Ciamician" dell'Università di
Bologna

and

Centro di Studio per la Fisica delle Macromolecole del C.N.R.
Via Selmi 2, 40126 Bologna, Italy

ABSTRACT

The miscibility of melt processed blends of bacterial poly(3-hydroxybutyrate) (PHB) with poly(epichlorohydrin) (PEC) is investigated over the whole range of compositions by means of differential scanning calorimetry, dynamic-mechanical analysis, and hot-stage optical microscopy. PHB and PEC are miscible in the melt in all proportions. After melt quenching, PHB/PEC blends show a single glass transition that linearly changes with composition between the T_gs of the pure components (PHB = 2°C, PEC = −21°C). At room temperature all PHB/PEC blends are partially crystalline, owing to crystallization of a constant fraction (58%) of the PHB present in each blend. A space-filling spherulitic morphology develops upon blend crystallization from the melt. Isothermal crystallization measurements show that over the range of crystallization temperatures (40°C < T_c < 130°C) and compositions (20% < PEC < 80%) explored, the spherulite radial growth rate (G) decreases with increasing PEC content. Biodegradation experiments, carried out in activated sludge and in enzymatic solution (PHB-depolymerase from *Aureobacterium saperdae*) on the blend containing 80% PHB, show both weight loss and surface erosion. The biodegradation results are discussed in terms of PHB chain-mobility.

INTRODUCTION

Poly(3-hydroxybutyrate), PHB, is accumulated intracellularly in the form of granules by a large number of microorganisms as a carbon and energy storage material [1]. Much attention was recently devoted to PHB and to the family of related poly(hydroxyalkanoates), PHA, on account of their biodegradability and biocompatibility. Various applications in agricultural, marine, and medical fields were proposed for bacterial polyesters [2]. They were also considered in a number of investigations as components of binary polymer blends, whose miscibility and physical properties were recently reviewed [3].

Atactic poly(epychlorohydrin), PEC, is an important industrial elastomer. Fernandes et al. [4] investigated the miscibility of PEC with aliphatic polyesters and showed that—independent of the presence of side chains or saturated cycles in the repeating unit of the polyester—miscible blends were formed when the ratio (N) of aliphatic carbons to ester groups was $2 < N < 10$. The bacterial polyester PHB has $N = 3$ and is expected to be miscible with PEC; preliminary indications of miscibility were reported in an earlier investigation [5].

In recent years a number of blends of PHB with highly substituted cellulose esters (CE) were investigated [6–9]; the blend components were found to be miscible in all proportions in the melt [6, 7], and upon solidification from the melt the blends showed well-defined spherulitic morphologies [9]. A biodegradation study [10] was conducted in activated sludge over a period of 12 months on a PHB/CE blend containing 20% CE (cellulose acetobutyrate with total degree of substitution 2.94). No evidence of biodegradation of the PHB-rich blend (neither weight loss nor surface erosion) was obtained after 12 months in an environment where plain PHB completely biodegraded in less than 20 days. Nonbiodegradability of the PHB/CE blend was tentatively attributed [10] to a detrimental decrease of PHB chain mobility, arising from mixing with the high-T_g cellulose ester.

If confirmed to be totally miscible with PHB, poly(epychlorohydrin) (with T_g lower than that of PHB, $-21°$ vs $+2°C$) appears as the ideal second component in a study of the influence of chain mobility on biodegradability of PHB-containing blends.

This work investigates the miscibility of PHB with PEC over the whole range of compositions by means of differential scanning calorimetry, dynamic mechanical analysis, and hot-stage optical microscopy. The results of biodegradation experiments—performed by exposing PHB-rich blends with well-defined morphologies to activated sludge and to a PHB-depolymerase solution—are discussed in terms of PHB chain mobility.

EXPERIMENTAL

Materials

Bacterial poly(3-hydroxybutyrate), PHB, is an ICI product (GO8, $M_n = 5.39 \times 10^5$, $M_w/M_n = 4.1$). Poly(epichlorohydrin), PEC, was purchased from Aldrich (Aldrich catalogue: average M_w ca. 700,000). Purification of PEC was carried out through dissolution in dichloromethane and elimination of impurities by filtration. Solvent evaporation was carried out in a Rotavapor; the polymer was subsequently stored in an oven under vacuum at 150°C for 24 hours in order to eliminate residual solvent.

Blend Preparation

Owing to the impossibility to "dry blend" the two components prior to melt processing (PHB is a powder whereas PEC is a bulky rubber), the following preliminary blending procedure was adopted; weighed amounts of PHB and PEC (weight ratio from 90/10 to 10/90 in 10% increments) were dissolved in dichloromethane (4% w/v solutions) and poured into glass petri dishes. PHB/PEC blends in the form of films were obtained by solvent evaporation, followed by vacuum drying overnight.

Either of the following melt processing procedures was applied to the solution-cast blend films: 1) the films were inserted between two aluminum plates containing a Teflon spacer and were compression molded using a Carver C12 laboratory press by heating at 195°C for 1.5 minutes under a pressure of 1 ton/m^2. Cooling to room temperature was performed through the press built-in water circuit. The thickness of compression-molded films was 0.11–0.12 mm. 2) The solution-cast films were introduced in the preheated (T = 195°C) mixing cup of a miniature mixing–injection molding machine and, after 1.5 minutes of melt processing, the blends were injection molded in the form of small bars ($30 \times 7.5 \times 1.5$ mm^3) and quenched in liquid nitrogen to facilitate release from the mold. Both processing conditions [compression molding (C.M.) and injection molding (I.M.)] were also applied to the pure component polymers. All samples were allowed to age at room temperature for at least 3 weeks before testing.

Experimental Methods

Calorimetric (DSC) measurements were carried out by means of a Dupont 9900 Thermal Analyser; the temperature scale was calibrated with high purity standards. PHB/PEC blends as well as the pure components were subjected to the following thermal cycle: 1) heating from −50 to 220°C at 20 deg/min (1st scan); 2) quenching to −80°C; 3) heating from −80 to 220°C at 20 deg/min (2nd scan). The melting and crystallization temperatures (T_m, T_c) were taken at the peak of the endotherm and exotherm respectively, while the glass transition temperature (T_g) was taken at the midpoint of the stepwise increase of the specific heat. Dynamic-mechanical measurements were performed on I.M. samples with a DMTA (Polymer-Laboratories Ltd.) operated in the dual cantilever blending mode at a frequency of 3 Hz and a heating rate of 3 deg/min. The temperature range investigated was from −100 to 100°C.

Measurements of the radial growth rate of spherulites were carried out with a Zeiss Axioscop polarizing optical microscope, equipped with a Linkam TH 600 hot stage. Isothermal crystallization measurements were performed on a thin slice of the I.M. samples, inserted between two microscope cover-glasses, and subjected to the following thermal program: heating at 20 deg/min up to 180°C (where the melt was squeezed into a film through a small pressure applied to the upper glass), then at 10 deg/min up to 195°C, followed by rapid quenching by means of N_2 gas flow (cooling rate > 250 deg/min) to the selected crystallization temperature (T_c), where isothermal crystallization was carried out. The whole procedure was performed without removing the sample from the hot stage. A videocamera, attached to the microscope through the Linkam VTO232 interface, allowed real time measurement of the spherulite dimensions after calibration with a micrometric reticule. A new sample was used for each crystallization measurement. Growth of four different spherulites (20-25 radius measurements each) was typically monitored at each T_c. Linear radius vs time behaviors were obtained, and the correlation coefficient of the linear regression through the results was always better than 0.999.

Biodegradation Experiments

Biodegradation experiments were carried out in activated sludge at the municipal wastewater treatment plant of Bologna (Italy) as previously described [10]. Over 1 year the largest pH and temperature fluctuations were 7-8 and 15-21°C respectively. Sterile controls were run in identical conditions using sterilized sludge.

Biodegradation experiments were also carried out at 37°C on ($10 \times 10\ \mathrm{mm}^2$) C.M. films, using a solution of PHB-depolymerase (7,5 μg/ml) purified from *Aureobacterium saperdae* [11] in potassium phosphate buffer (100 mM, pH 7) with 8% ethylene glycol as enzyme stabilizer. For each exposure interval (20 hours), fresh enzymatic solution was used.

Film surfaces were examined before and after biodegradation experiments using a scanning electron microscope (Philips 515); samples were sputter-coated with gold.

RESULTS AND DISCUSSION

Calorimetric Analysis

PHB/PEC blends with PHB content from 10 to 90% were investigated by DSC. In the 1st scan all blends showed a melting endotherm whose temperature (T_m) and associated enthalpy (ΔH_m) decreased with increasing content of amorphous component (PEC). It is worth remarking that crystallinity is present even in the blend containing as little as 10% PHB. The values of T_m and ΔH_m are collected in Table 1 and refer to compression-molded (C.M.) samples. Figure 1 shows that the melting enthalpy linearly depends on composition and suggests that the fraction of PHB which crystallizes in each blend remains constant and equal to the crystalline content of the pure biopolymer (58%, from comparison with the literature value [12] for 100% crystalline PHB).

In miscible blends, the melting point depression can be described by means of an equation developed by Nishi and Wang [13]:

$$\frac{1}{T_m} = \frac{1}{T_m{}^{\circ}} - (R/\Delta H_u)(V_2/V_1)\chi_{12}(\phi_1)^2 \tag{1}$$

where 1 and 2 indicate the amorphous and crystalline components respectively, T_m and $T_{m^{\circ}}$ are the melting temperatures of the blend and of the pure cyrstallizable polymer, V is the repeating unit molar volume, ΔH_u is the repeating unit melting

TABLE 1. Melting Temperature and Enthalpy of PHB/PEC Blends (from 1st DSC scan on compression-molded samples)

PHB/PEC	T_m, °C	ΔH_m, J/g
10/90	149	10
20/80	155	17
30/70	160	26
40/60	163	32
50/50	168	45
60/40	170	51
70/30	171	58
80/20	173	67
90/10	174	76
100/0	175	84

enthalpy, ϕ is the volume fraction, and χ_{12} is the Flory-Huggins (polymer-polymer) interaction parameter. If the binary blend is miscible, by plotting $1/T_m$ as a function of $(\phi_1)^2$ a linear behavior should be obtained. An approximation commonly introduced in Eq. (1) regards the use of weight (w_1) instead of volume fraction (ϕ_1). In the present case, substitution of ϕ_1 by w_1 in Eq. (1) is reasonable since the densities of amorphous PHB [12] and PEC [4] at room temperature are similar, and all amorphous polymers are commonly assumed to have an analogous volume expan-

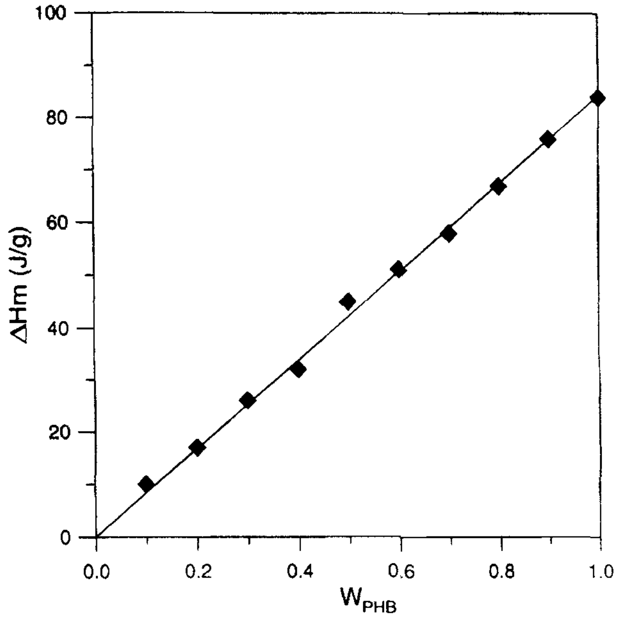

FIG. 1. Melting enthalpy of PHB/PEC blends as a function of PHB weight fraction.

sion coefficient (about 6 × 10^{-4}°K^{-1} [14]). The T_m results of Table 1, plotted according to Eq. (1), are shown in Fig. 2. From the slope of the linear regression through the experimental data, the interaction parameter χ_{12} can be calculated. By using $\Delta H_u = 12.6$ kJ/mol [12], $V_2 = 73.14$ cm^3/mol for PHB [12], and $V_1 = 68.03$ cm^3/mol for PEC [4], the negative value $\chi_{12} = -0.23$ is obtained, which suggests that mixing of PHB with PEC is promoted by efficient polymer-polymer interactions.

The interaction energy density [13] of the polymer-polymer pair [$B = (\chi_{12}RT_m)/V_1$] is -12.6 J/cm^3 for the present PHB/PEC blends, a result that very well fits into the trend of experimental B values for miscible polyester/PEC blends reported by Fernandes et al. [4] as a function of the ratio (N) of aliphatic carbons to ester groups in the polyester. In particular, PHB/PEC blends have the same value of B as blends of PEC with poly(ethylene adipate), a polyester with $N = 3$ like PHB.

DSC curves of PHB/PEC blends and of the pure polymers after melt quenching (2nd scan) are collected in Fig. 3. A glass transition, whose temperature gradually decreases with increasing PEC content, is observed in all curves. In blends with PHB content ≥30%, at temperatures higher than T_g the DSC curve shows a crystallization exotherm associated with PHB crystallization from the rubbery state (cold crystallization). This crystalline phase melts at a temperature which clearly decreases with increasing PEC content in the blend, in agreement with the results of the 1st DSC scans previously discussed (see Table 1). Glass transition, crystallization, and melting temperatures (T_g, T_c, and T_m), specific heat increment at T_g (Δc_p),

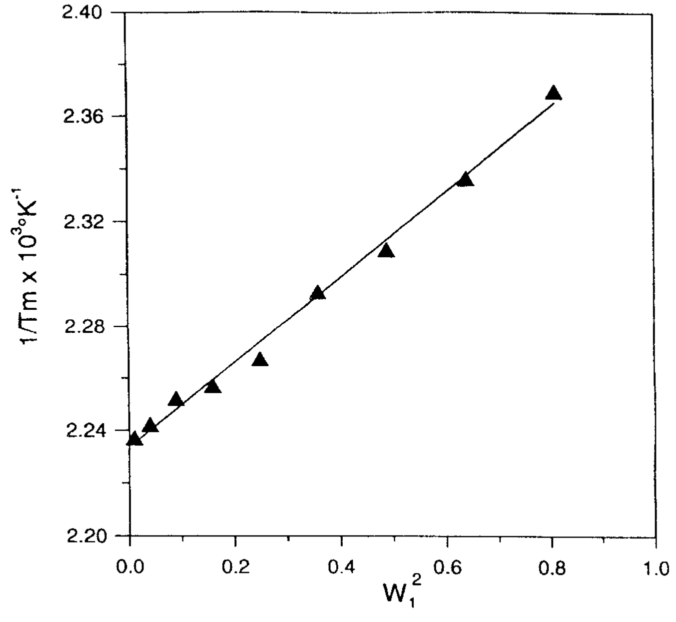

FIG. 2. Melting temperature (T_m) of PHB/PEC blends plotted according to Eq. (1) with w_1 instead of ϕ_1.

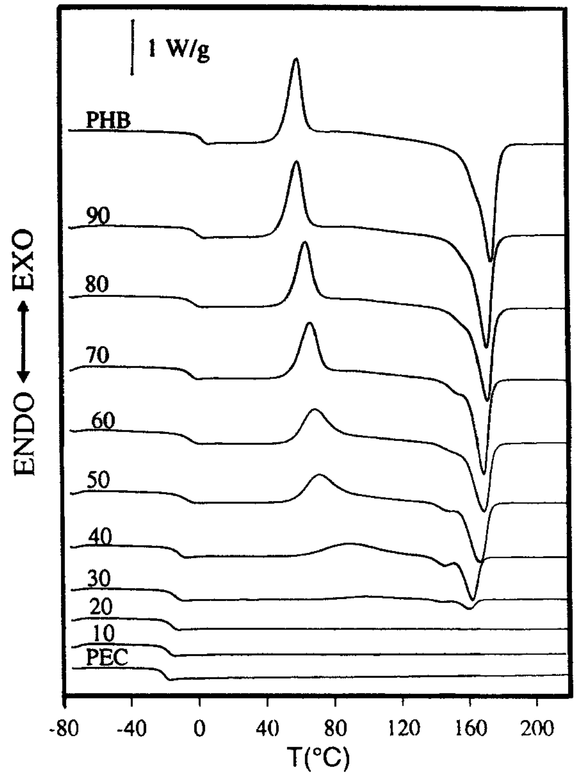

FIG. 3. DSC curves of PHB/PEC blends (compression-molded samples) after melt quenching. PHB weight percent is indicated on curves.

and crystallization and melting enthalpies (ΔH_c and ΔH_m), taken from the curves of Fig. 3, are collected in Table 2.

As described in the Experimental Section, PHB/PEC blends were prepared in two different ways (compression or injection molding). The influence of processing on blend properties was investigated by comparing DSC results on C.M. and I.M. blends, as shown in Fig. 4. The excellent agreement of T_m and T_g values for the two series of blend samples demonstrates identity of phase behavior, independent of the preparation procedure employed. On the basis of this result, DSC, DMTA, and biodegradation data can be safely correlated regardless of the type of test specimen used (I.M. in DMTA, C.M. in biodegradation experiments in order to maximize the exposed surface).

The T_g behavior of PHB/PEC blends in Figure 4 confirms the conclusion already drawn from the melting results, i.e., that the two polymers are miscible in all proportions in the melt. Upon quenching the melt to low temperature, a mixed glass is obtained which undergoes the glass-to-rubber transition at a temperature intermediate to those of the pure components. T_g changes linearly with composition, as is frequently found in miscible blends of polymers whose T_gs do not differ much (in this case, $T_{g_2} - T_{g_1} = 23°C$). Moreover, since T_g of all PHB/PEC blends lays

TABLE 2. Calorimetric Properties of Melt-Quenched PHB/PEC Blends (from 2nd DSC scan on compression-molded samples)

PHB/PEC	T_g, °C	Δc_p, J/g · °C	T_c, °C	ΔH_c, J/g	T_m, °C	ΔH_m, J/g
0/100	−21	0.63	–	–	–	–
10/90	−19	0.60	–	–	–	–
20/80	−17	0.59	–	–	–	–
30/70	−14	0.62	98	5	160	7
40/60	−13	0.56	90	26	163	25
50/50	− 8	0.59	72	40	167	44
60/40	− 6	0.58	70	47	169	49
70/30	− 5	0.62	67	56	169	58
80/20	− 3	0.59	64	61	171	63
90/10	0	0.59	59	69	171	75
100/0	2	0.60	59	76	174	80

below room temperature, it is reasonable that during room temperature storage partial crystallization of PHB occurs over the whole composition range (see Table 1).

Dynamic Mechanical Analysis

Room-stored partially crystalline PHB/PEC blends were investigated by dynamic mechanical analysis. The DMTA curves of PHB/PEC blends and of the neat polymers are shown in Fig. 5. The totally amorphous character of PEC is clearly revealed by the catastrophic drop of the elastic storage modulus (E') at the glass transition (more than three orders of magnitude). In contrast, in all PHB/PEC blends, E' above the glass transition remains sensibly higher than in pure PEC. From the DSC results it is known that the blends are miscible and that they all contain a crystalline phase. Therefore, above T_g the blends are two-phase systems composed of a rigid phase (crystalline PHB) and a soft phase (amorphous PHB and PEC in a mixed rubbery state). It is interesting to compare the experimental values of E' (from the curves of Fig. 5) at a selected temperature above T_g (25°C) with the predictions of a simple model [15] describing the elastic modulus (E) of two-phase composites as a function of composition and of phase arrangement. The model contemplates two limiting cases where the stiff and soft phases (with moduli E_1 and E_2 respectively) are connected either in parallel

$$E = E_1 w_1 + E_2 w_2 \tag{2}$$

or in series

$$\frac{1}{E} = \frac{w_1}{E_1} + \frac{w_2}{E_2} \tag{3}$$

In order to compare the predictions of Eqs. (2) and (3) with the experimental results for PHB/PEC blends, reasonable values must be assigned to E_1 and E_2. Using as the elastic modulus of the soft phase (E_2) the experimental value of PEC at

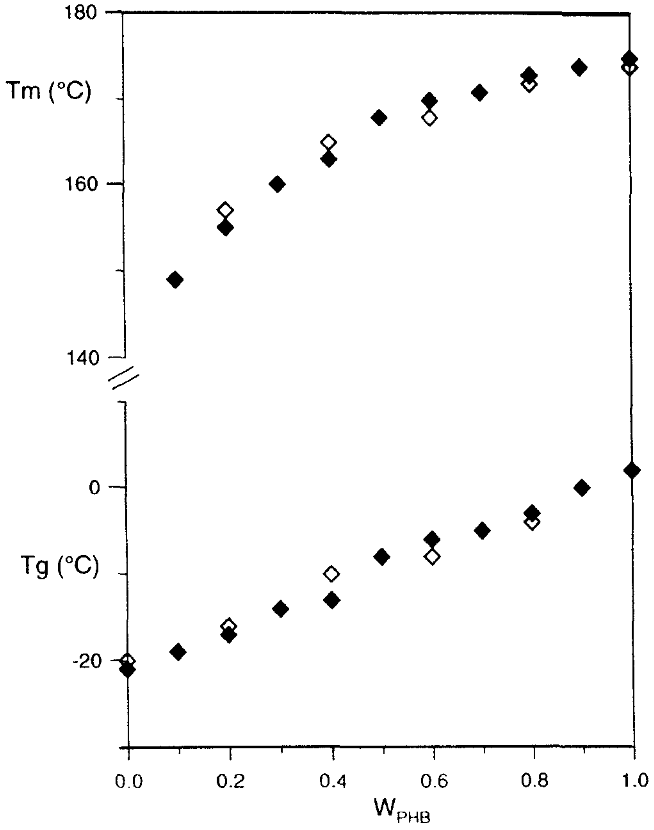

FIG. 4. Composition dependence of melting temperature T_m (from 1st DSC scan) and glass transition temperature T_g (from 2nd DSC scan) of PHB/PEC blends: compression-molded (◆) and injection-molded (◇) samples.

25 °C and for the rigid phase (E_1)—assuming that the moduli of crystal and glass do not differ much—the experimental value of partially crystalline PHB below T_g [log E' (Pa) = 9.8], the curves drawn in Fig. 6 as a continuous (Eq. 2) and a broken line (Eq. 3) are obtained.

Also shown in Fig. 6 are the experimental log E' results for the blends at 25 °C (taken from Fig. 5) as a function of the rigid phase content (crystalline PHB) in each blend. Calculation of the crystalline content of PHB/PEC blends is straightforward since from DSC (Fig. 1) it is known that it constitutes a constant fraction (58%) of the overall PHB content of the blend. Inspection of Fig. 6 shows that PHB/PEC blends have elastic moduli much closer to the upper than to the lower curve. The experimental E' value at 25 °C of plain, partially crystalline PHB, shown in Fig. 6 as an open symbol at 58% crystallinity, closely matches the predictions of the model for phases connected in parallel (Eq. 2). Notably, small amounts of crystalline PHB lead to an increase of E' of two orders of magnitude. This suggests that the crystals tend to form a practically continuous phase (parallel model).

In the DMTA curves of Fig. 5 the loss modulus (E'') shows a relaxation peak at the glass transition whose temperature (T_α) increases in the blends with increasing

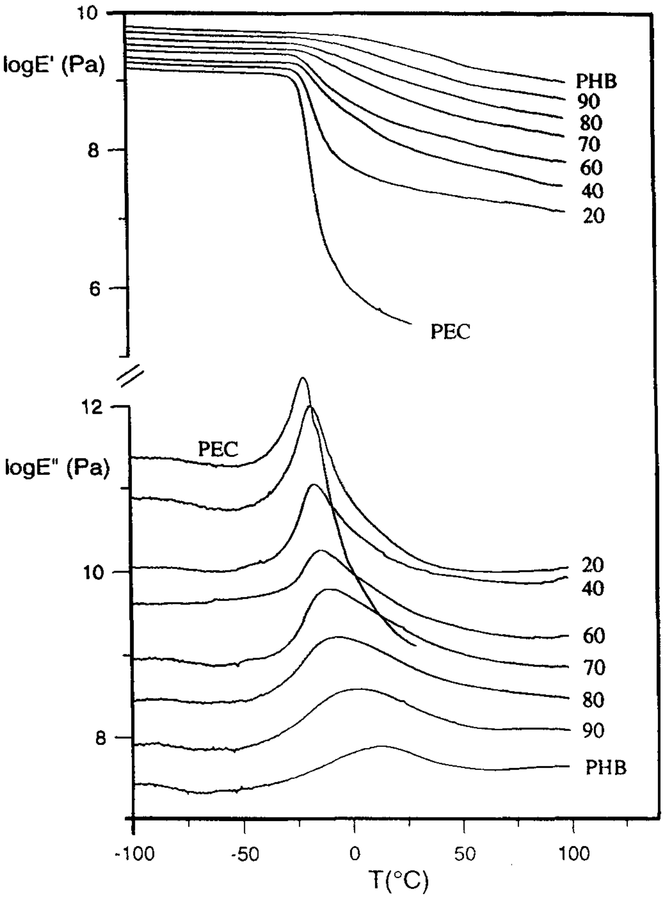

FIG. 5. Dynamic mechanical curves of PHB/PEC blends. For the sake of clarity the loss modulus (E'') curves are vertically shifted (the scale refers to blend 90/10). PHB weight percent is indicated on curves.

content of the high-T_g component (PHB). It has been suggested [16] that in amorphous polymers the T_g determined by DSC roughly corresponds to T_α obtained from the E'' vs T curve at frequencies around 1 Hz. On account of the rather low operating frequency of the present DMTA measurements (3 Hz), DSC and DMTA results on PHB/PEC blends can be reasonably compared, provided it is remembered that T_gs by DSC refer to melt quenched totally amorphous samples while T_αs by DMTA are obtained on partially crystalline blends. Since the amount of crystalline PHB in each blend is known, the actual composition of the amorphous phase in the crystalline blends used in DMTA measurements can be easily calculated and is reported in Table 3.

Figure 7 compares T_g (by DSC on I.M. samples) with T_α for the various PHB/PEC blends. T_α is plotted as a function of the "true" composition of the amorphous phase taken from Table 3, whereas the overall composition is used when plotting T_g. It is seen that the T_α values follow the linear dependence on composition of the

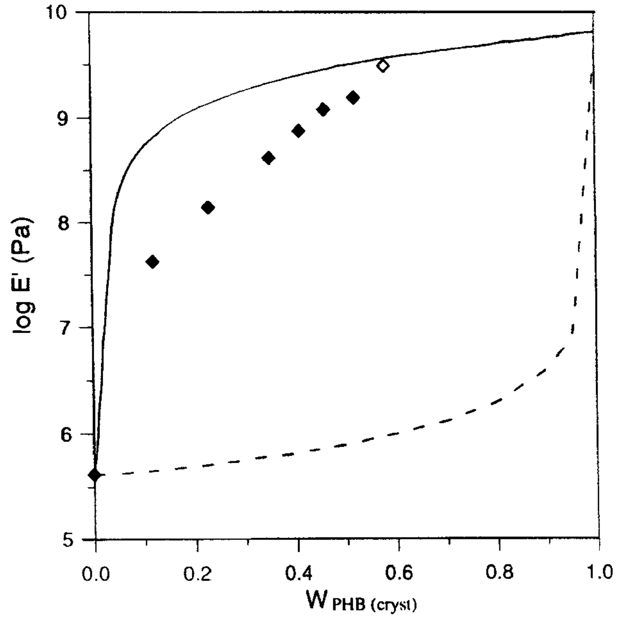

FIG. 6. Elastic storage modulus (E') at 25°C of PHB/PEC blends (from Fig. 5) as a function of crystalline PHB content. Continuous curve: Eq. (2); broken curve: Eq. (3).

DSC T_gs except for the blend with overall composition 90/10 (amorphous phase composition 79/21) where T_α lays well above T_g. This difference is attributed to the high fraction of crystalline material present in this blend, where the many existing crystals provide anchoring sites to the disordered PHB chain segments, leading to a substantial decrease of the amorphous phase mobility. As a consequence (see Fig. 5), the glass transition relaxation broadens and T_α increases. For the same reason, in Fig. 7, T_α of partially crystalline plain PHB is so much higher than T_g of the totally amorphous quenched biopolymer. Although all PHB/PEC blends investi-

TABLE 3. Overall Blend Composition, Composition of the Amorphous Phase, and T_α (from DMTA) of Partially Crystalline PHB/PEC Blends

Overall PHB content, %	PHB content in amorphous phase, %	T_α, °C
0	0	−21
20	10	−19
40	22	−17
60	39	−14
70	49	−11
80	63	− 7
90	79	2

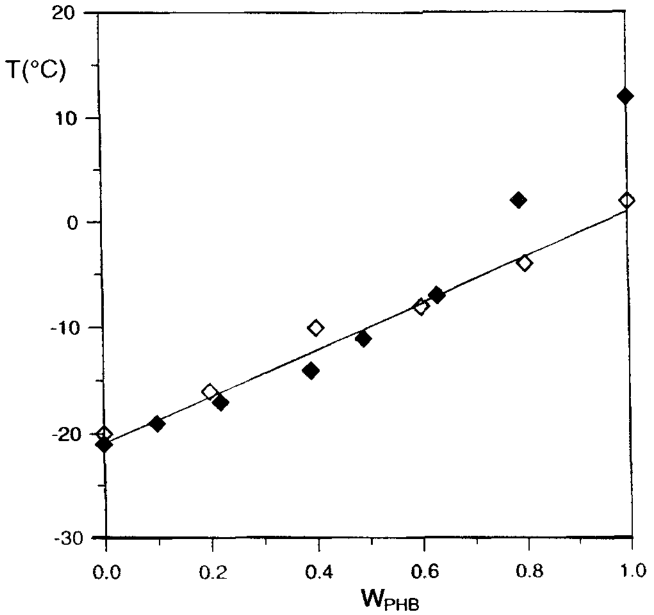

FIG. 7. T_g from DSC (◇) and T_α by DMTA (◆) of PHB/PEC blends as a function of composition (see text).

gated are partially crystalline, the results of Fig. 7 indicate a relevant physical crosslinking effect on T_α only in the blend with the highest PHB content (90%).

Isothermal Crystallization

Isothermal crystallization measurements were carried out on PHB/PEC blends containing 20, 40, and 80% PEC over a wide range of temperatures (40°C $< T_c <$ 130°C). The three blends investigated developed a spherulitic morphology over the whole range of T_cs explored. The spherulites were space-filling and grew linearly with time. The rate of spherulite growth in blends at a given temperature is primarily governed by the composition of the melt at the growing lamellar front, and a steady-state growth indicates constancy of melt composition [17]. Figure 8 shows the morphology of PHB/PEC blends containing 20 and 80% PEC after isothermal crystallization at 80°C. As already found in other miscible PHB-based blends [9, 18, 19], when the PHB content is high (see blend 80/20) the spherulites maintain the banded appearance associated with regular lamellar twisting during growth, typical of the pure biopolymer. More surprising is the observation that even when the crystallizable component amounts to a mere 20%, a quite regular spherulitic morphology develops (note in Fig. 8b the evident Maltese cross and the well-defined linear boundary at the impinging front).

The spherulitic radial growth rate (G) was calculated from the slope of the linear dependence of the spherulite radius vs time at the different crystallization temperatures. Figure 9 shows G as a function of T_c for the three blends examined (pure PHB is included for the sake of comparison). In all blends G increases with

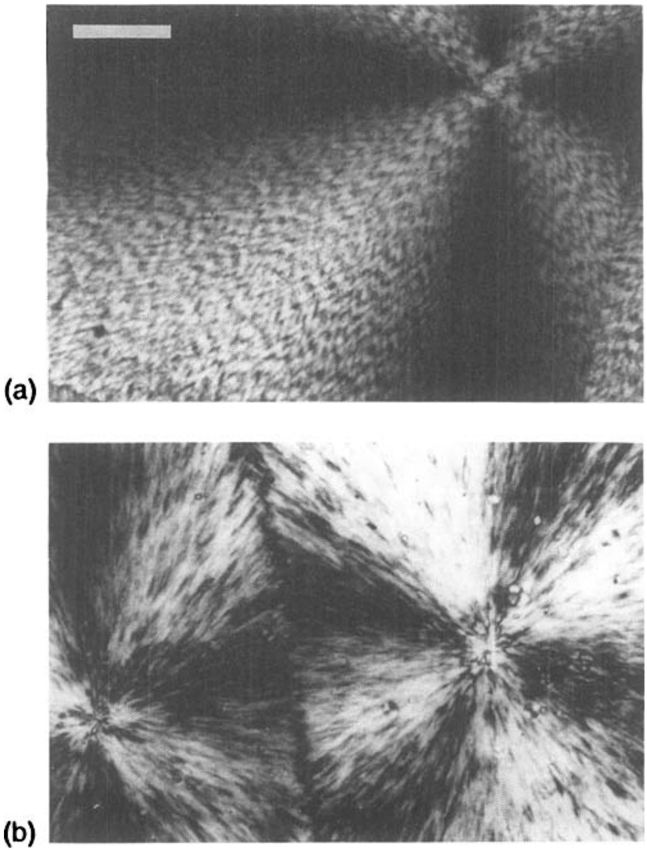

FIG. 8. Optical micrographs (same magnification) of PHB/PEC blends isothermally crystallized at T_c = 80°C: (a) 80/20; (b) 20/80. Bar = 0.1 mm.

T_c up to a maximum, then decreases, following a trend well-established in pure polymers.

The presence of the second polymeric component in PHB/PEC blends significantly reduces the rate of PHB crystallization: at all T_cs, G decreases with increasing PEC content in the blend. When the amount of PEC reaches 80%, G is 1.5 orders of magnitude lower than in pure PHB. This is a very significant crystallization rate depression, although remarkably less than found in other miscible PHB-based blends (namely blends with cellulose esters) [9].

To a first approximation, when a polymer crystallizes from a homogeneous melt containing a noncrystallizable polymer, four main factors [20, 21] can be considered responsible for the crystallization rate changes observed with increasing amorphous polymer content: 1) a "dilution effect" that reduces the number of crystallizable segments at the growing lamellar front, 2) the presence of noncrystallizable material at the lamellar tip that must diffuse away to allow crystal growth, 3) melting point depression that reduces the driving force to crystallization, and 4) T_g changes upon blending which modify the rate of transport of the crystallizable segments across the liquid-solid interface. While factors 1) to 3) should always lead

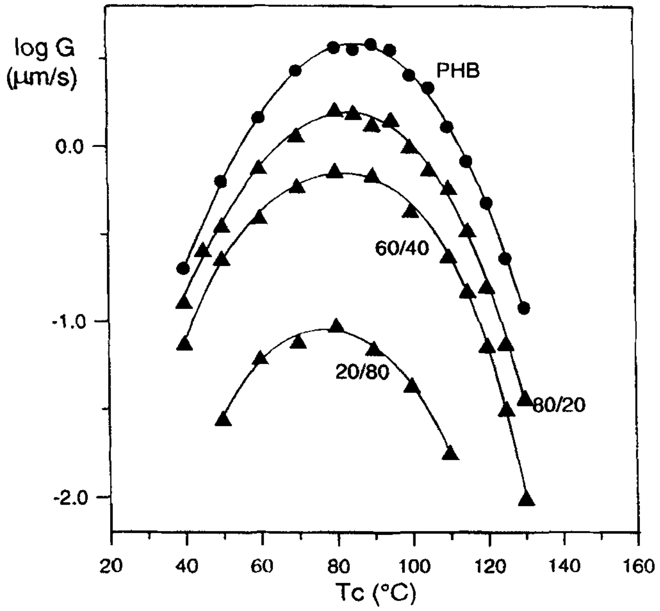

FIG. 9. Radial growth rate (G) as a function of crystallization temperature (T_c) for PHB (●) and PHB/PEC blends (▲, composition indicated).

to a decrease of G with increasing content of noncrystallizable component, the effect of factor 4) depends on whether $T_{g_{blend}}$ is higher or lower than that of the pure crystallizable polymer. In the former case, i.e., when the amorphous polymer is the high-T_g component of the blend, factor 4) negatively contributes to G, further lowering the crystallization rate. Conversely, if $T_{g_{blend}}$ is always lower than T_g of the plain crystalline polymer—like in PHB/PEC blends—a positive contribution to G is expected from factor 4).

The G vs T_c behaviors of Fig. 9 show a remarkable crystallization rate reduction with increasing PEC content over the whole T_c range explored. This implies a strong influence of the above mentioned G-depressing effects [factors 1) to 3)] and a modest opposite contribution of factor 4). The latter result is quite reasonable in the case of PHB/PEC blends, where mobility of PHB segments across the liquid-solid interface during crystallization cannot be much enhanced by the rather small T_g changes shown in Fig. 4.

Finally, the G vs T_c curves in Fig. 9 are seen to shift slightly to lower temperatures with increasing PEC content in the blend. This observation can be easily rationalized by remembering that T_g and T_m represent the lower and upper limits of the temperature range where crystallization can occur and considering that both values decrease with increasing PEC concentration (see Tables 2 and 3).

All the experimental evidence collected so far (by DSC, DMTA, and isothermal crystallization measurements) demonstrates complete miscibility of PHB with PEC in the melt. When PHB/PEC blends are cooled from the melt, the solidification process involves formation of well-defined spherulitic morphologies. Optical microscope observations show that the spherulitic texture develops not only during isothermal crystallization (where the spherulite size is rather homogeneous) but also upon uncontrolled cooling to room temperature after melt processing (where a broader spherulite size distribution is obtained).

Biodegradation

A PHB/PEC blend containing 80% PHB (C.M. film) was selected for biodegradation experiments in activated sludge. The choice was suggested by the high content of biodegradable component of this blend and by the intention to compare the biodegradation results with those previously obtained [10] on a blend of PHB with a cellulose ester (PHB/CE) with the same composition. Both the PHB/PEC blend presently investigated and the mentioned PHB/CE blend are fully miscible in the melt and show spherulitic morphology with impinging spherulites in the solid state. Hence the spherulite skeleton is constituted of PHB lamellar crystals whereas the space between lamellae (or lamellar bundles) is occupied by a homogeneous amorphous mixture of PHB and the other blend component.

Biodegradation experiments were conducted in activated sludge on the PHB/PEC blend as well as on plain PHB and PEC. In agreement with previous results [10], compression-molded films of pure PHB completely biodegraded in less than 20 days. Conversely, plain PEC showed no evidence of degradation after 10 months of sludge exposure. Sterile controls (blend and pure components) were run for 4 months and showed neither weight loss nor surface erosion.

The PHB/PEC blend was exposed to activated sludge for different times up to a maximum of 4 months. Figure 10 shows SEM micrographs of the blend surface before (a) and after exposure (b and c). Apart from striations caused by scratches on the Teflon molding plates, the original (undegraded) film surface (a) is flat. After sludge exposure (b and c), the surface becomes rough with clear signs of erosion (biodegradation). Unlike pure PHB [10], in the blend the biodegradation phenomenon does not uniformly involve all the exposed surface (see b), but rather appears to be localized in selected areas where bacterial colonies have succeeded in settling. Multiple examinations of film surfaces after different exposure times showed that the eroded areas—localized and rather limited at first—tend to spread over the surface as exposure time increases. After 4 months in sludge, only a few scattered nondegraded patches, such as the area shown in micrograph b), remain on the surface.

The effects of bacterial attack are more evident in areas where small spherulites concentrate than in areas with spherulites of larger dimensions; as an example, micrograph c) shows large spherulites still retaining the marks of the mold (little or not attacked at all) surrounded by extensively eroded smaller ones. In a recent paper [22] it was shown that in plain PHB films subjected to biodegradation by a purified enzyme solution, the impinging spherulite fronts exposed on the surface undergo preferential degradation. This observation was attributed to accumulation of chain segments in disordered conformations at the spherulite boundaries. Micrograph c) in Fig. 10 also suggests that in the blend the enzymes secreted by the sludge microorganisms preferentially attack the spherulite boundary and that biodegradation subsequently proceeds to the remaining portion of the exposed spherulite. Hence it is reasonable that those parts of the surface containing spherulites of small

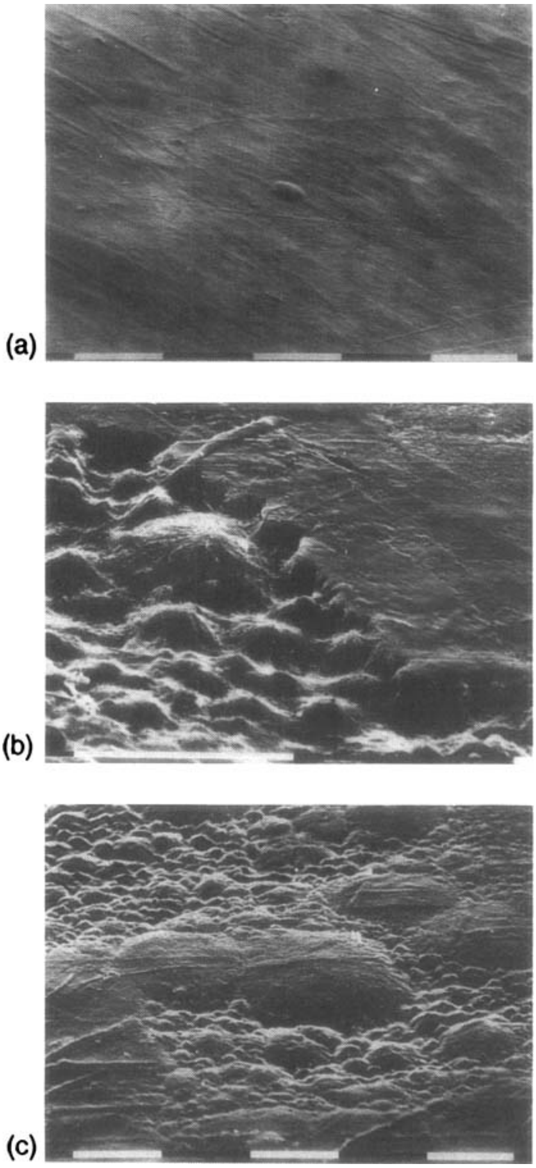

FIG. 10. SEM micrographs of the surface of PHB/PEC (80/20) blend: (a) before and (b and c) after 4 months of exposure to activated sludge. Bar = 0.1 mm.

average size are more extensively biodegraded than regions where spherulites of larger dimensions are located.

Figure 11(a) shows a magnification of the biodegraded surface of the PHB/PEC blend where eroded spherulites of varying dimensions are clearly observed. For the sake of comparison, Fig. 11(b) shows the surface of a compression-molded PHB film after 4 days of sludge exposure. A spherulitic texture is observed in both micrographs of Fig. 11, but closer inspection reveals substantial differences in the

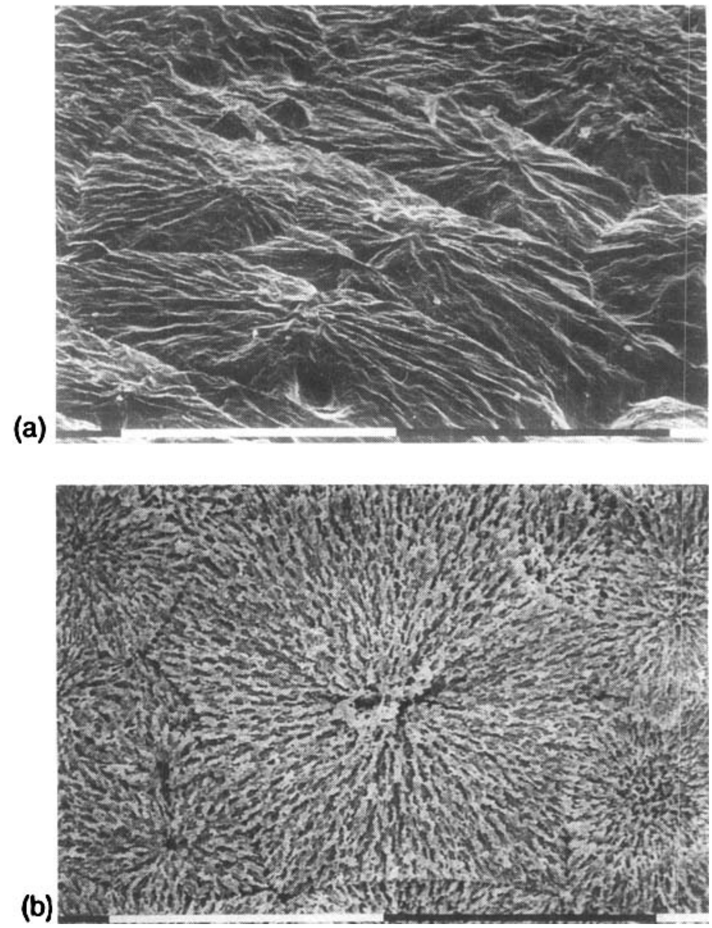

FIG. 11. SEM micrographs of the surface of PHB/PEC (80/20) blend after 4 months in activated sludge (a) and of PHB after 4 days in activated sludge (b). Bar = 0.1 mm.

biodegraded surface of the pure polymer and of the blend. In micrograph b), bundles of sharp crystalline PHB lamellae (naked of the fast degrading amorphous phase) are seen all over the surface, in agreement with previous observations [10]. In contrast, no sharp edges are observed in the ribbons that radiate from the spherulite center in the micrograph of the biodegraded blend surface (a). Also, they appear to be thicker than the lamellae observed on the degraded plain PHB surface [magnification in micrographs a) and b) is the same]. To a first approximation it is suggested that the radial ribbons on the degraded blend surface are composed of rubbery PEC that was originally located between the spherulite lamellae and was left behind upon biodegradation of the PHB component.

The PHB/PEC blend was also subjected to biodegradation in enzymatic solution, using a purified PHB-depolymerase from *Aureobacterium saperdae* [11]. Figure 12 shows the weight loss per unit exposed area ($\Delta m/S$) as a function of exposure time for the 80/20 blend. $\Delta m/S$ for plain PHB is also shown for the sake of

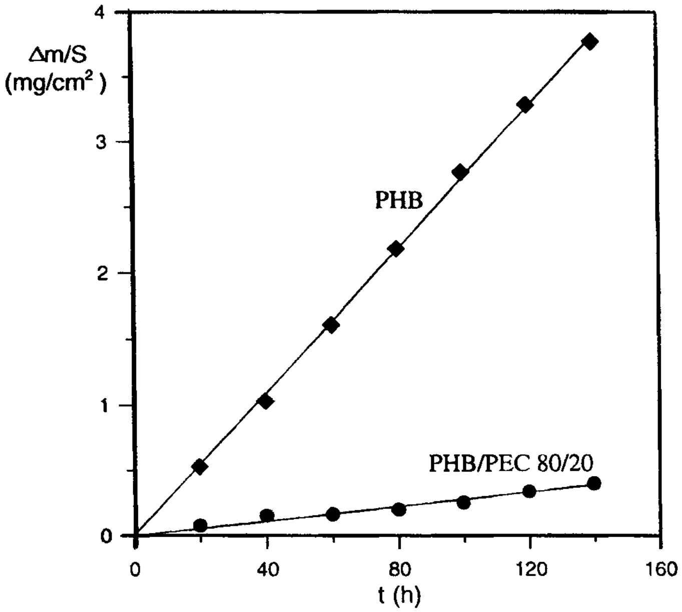

FIG. 12. Weight loss per unit exposed area (Δ*m*/*S*) of PHB/PEC (80/20) blend and of plain PHB as a function of exposure time to an aqueous solution of PHB-depolymerase from *Aureobacterium saperdae* at 37°C and pH 7.

comparison. The blend weight is seen to decrease in a regular fashion, but at a much slower rate than that of pure PHB (2.8×10^{-3} vs 2.7×10^{-2} mg/cm^2·h). Figure 13 compares the surfaces of PHB/PEC blend (a) and PHB (b) after biodegradation in enzymatic solution to the same value of Δ*m*/*S*. As already observed after biodegradation in activated sludge (compare with Fig. 11), the eroded surfaces of PHB and of the blend have a different appearance: the sharp protruding lamellae, typical of degraded PHB, are totally absent from the surface of the biodegraded blend, where the spherulitic morphology is partially dimmed by what seems to be a layer of nondegraded PEC.

CONCLUSIONS

The interesting result of this work is that the PHB/PEC blend containing 80% PHB biodegrades both in enzymatic solution and in activated sludge, whereas it was previously demonstrated [10] that a blend with the same composition and analogous spherulitic morphology containing a cellulose ester (acetate butyrate) does not biodegrade over a much longer period of sludge exposure (12 months). It is recalled that neither of the second blend components (PEC or CE) biodegrades in activated sludge. It is well established [10, 22, 23] that degradation in plain spherulitic PHB starts from the polymer chains in the disordered amorphous phase and sequentially proceeds to the exposed lamellar crystals. It can be easily calculated that crystalline PHB constitutes about 50% of the total mass of both PHB/PEC and PHB/CE

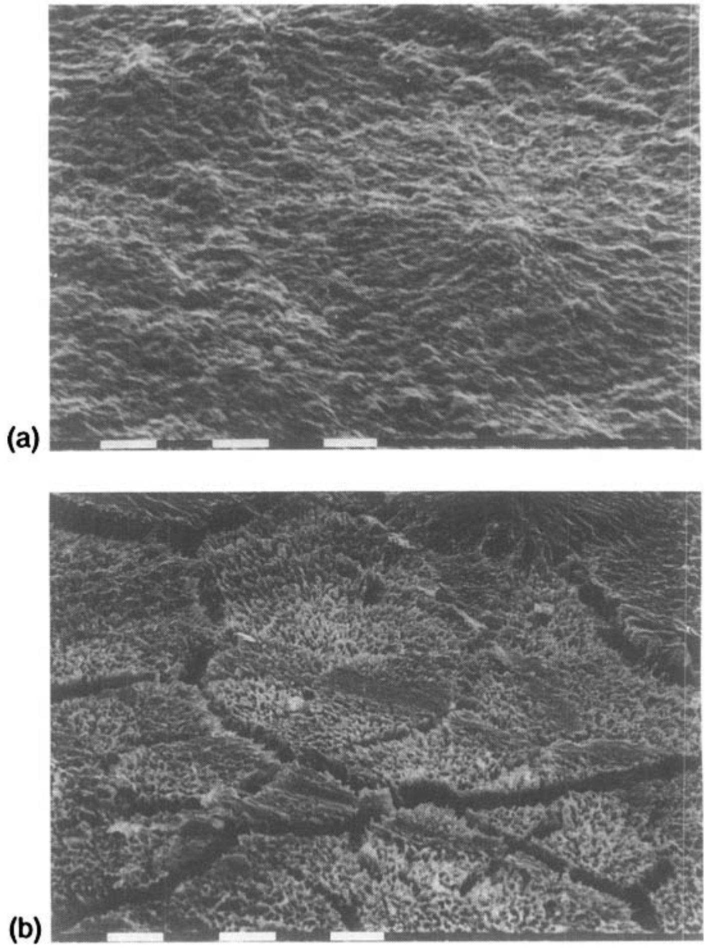

FIG. 13. SEM micrographs of the surface after biodegradation in enzymatic solution ($\Delta m/S$ = 0.4 mg/cm^2) of PHB/PEC (80/20) blend (a) and plain PHB (b). Bar = 0.01 mm.

(80/20) blends. Notwithstanding this large fraction of pure biopolymer phase, earlier evidence that the blend containing CE did not biodegrade over prolonged sludge exposure suggested [10] that attack to the lamellar PHB phase was conditioned by prior consumption of some interlamellar amorphous material, a process that was inhibited in the PHB/CE blend for some reason.

The present results may offer an explanation to the behavior observed in PHB/CE. It is recalled that the glass transition temperature of the second component in PHB/PEC and PHB/CE blends is very different (−21°C for PEC, +103°C for the CE). This entails that the interlamellar mixed phase in the two blends has different mobility at the temperature where the biodegradation experiments are carried out: in the blend with PEC, PHB chains in the amorphous phase are in a mobile rubbery state, whereas in the other blend their mobility is hindered by the high-T_g cellulose ester.

A critical analysis of the data available in the literature for *miscible blends* containing bacterial PHB substantiates the idea that when the amorphous phase retains its mobility, biodegradation of PHB-based blends can occur, while when such mobility is lost, enzymatic hydrolysis of PHB chains is totally inhibited. Apart from a few cases [24, 25] where the blending procedure (namely solution casting) induced partial phase separation of the PHB component and limited weight loss was observed in PHB-rich blends, to the best of our knowledge no papers in the literature report biodegradation of miscible blends of PHB with high-T_g polymers. Conversely, recent investigations [26, 27] on miscible blends of bacterial PHB with synthetic atactic PHB have demonstrated that enzymatic degradation occurs in blends where the second component has the same T_g as the biopolymer.

It is concluded that a necessary—though not sufficient—condition for the onset of PHB biodegradation in miscible blends is mobility of the PHB chain segments in the amorphous phase. This condition is fulfilled in blends where the other blend component has a glass transition temperature similar to—or lower than—that of the biopolymer.

ACKNOWLEDGMENTS

Special thanks are due to Dr. Patrizia Sadocco of Stazione Sperimentale per la Cellulosa, Carta e Fibre Tessili Vegetali e Artificiali, Milan, for the enzymatic biodegradation measurements. Thanks are also due to Antonietta Specchiulli for performing characterization experiments on the blends. This work was partially supported by the European Economic Community (Contract AIR2-CT93-1099).

REFERENCES

[1] Y. Doi, *Microbial Polyesters*, VCH Publishers, New York, NY, 1990.

[2] P. A. Holmes, in *Developments in Crystalline Polymers*, Vol. 2 (D. C. Basset, Ed.), Elsevier, New York, NY, 1988.

[3] H. Verhoogt, B. A. Ramsay, and B. D. Favis, *Polymer, 35*, 5155 (1994).

[4] A. C. Fernandes, J. W. Barlow, and D. R. Paul, *J. Appl. Polym. Sci., 29*, 1971 (1984).

[5] M. Tsukada, M. Romanò, and A. Seves, *Acta Polym., 43*, 327 (1992).

[6] M. Scandola, G. Ceccorulli, and M. Pizzoli, *Macromolecules, 25*, 6441 (1992).

[7] M. Pizzoli, M. Scandola, G. Ceccorulli, and U. Piana, *Book Abstr. 4th Eur. Symp. Polym. Blends*, Capri, 1993, p. 309.

[8] G. Ceccorulli, M. Pizzoli, and M. Scandola, *Macromolecules, 26*, 6722 (1993).

[9] M. Pizzoli, M. Scandola, and G. Ceccorulli, *Ibid., 27*, 4755 (1994).

[10] G. Tomasi and M. Scandola, *J. Macromol. Sci.—Pure Appl. Chem., A32*, 671 (1995).

[11] P. Sadocco, S. Nocerino, E. Dubini-Paglia, A. Seves, and G. Elegir, submitted to *J. Environ. Polym. Degrad.*

[12] P. J. Barham, A. Keller, E. L. Otun, and P. A. Holmes, *J. Mater. Sci.*, *19*, 2781 (1984).

[13] T. Nishi and T. T. Wang, *Macromolecules*, *8*, 909 (1975).

[14] D. W. Van Krevelen, *Properties of Polymers*, Elsevier, New York, NY, 1976.

[15] L. E. Nielsen, *Mechanical Properties of Polymers and Composites*, Vol. 2, Dekker, New York, NY, 1974, p. 397.

[16] L. E. Nielsen, *Ibid.*, Vol. 1, Dekker, New York, NY, 1974, p. 147.

[17] H. D. Keith and F. J. Padden, *J. Appl. Phys.*, *35*, 1270 (1964).

[18] M. Avella, E. Martuscelli, and P. Creco, *Polymer*, *32*, 1647 (1991).

[19] H. Abe, Y. Doi, M. M. Satkowski, and I. Noda, *Macromolecules*, *27*, 50 (1994).

[20] G. C. Alfonso and T. P. Russell, *Ibid.*, *19*, 1143 (1986).

[21] G. C. Alfonso, in *Interpretation of Fundamental Polymer Science and Technology*, Vol. 5 (P. J. Lemstra and L. D. Kleintjens, Eds.), Elsevier, London, 1991.

[22] G. Tomasi, M. Scandola, B. H. Briese, and D. Jendrossek, *Macromolecules*, *29*, 507 (1996).

[23] Y. Kumagai, Y. Kanesawa, and Y. Doi, *Makromol. Chem.*, *193*, 53 (1992).

[24] Y. Kumagai and Y. Doi, *Polym. Degrad. Stab.*, *36*, 241 (1992).

[25] D. F. Gilmore, R. C. Fuller, B. Schneider, R. W. Lenz, N. Lotti, and M. Scandola, *J. Environ. Polym. Degrad.*, *2*, 49 (1994).

[26] Y. Kumagai and Y. Doi, *Makromol. Chem., Rapid Commun.*, *13*, 179 (1992).

[27] H. Abe, I. Matsubara, and Y. Doi, *Macromolecules*, *28*, 844 (1995).

Received February 25, 1996